

CHARACTERISTICS OF DECAYING STORMS DURING LIGHTNING CESSATION AT KENNEDY SPACE CENTER AND CAPE CANAVERAL AIR FORCE STATION

Holly Anderson Melvin*, Henry E. Fuelberg
The Florida State University, Tallahassee, FL, USA

1. INTRODUCTION

Previous research has revealed many factors leading to lightning initiation [e.g., Workman and Reynolds, 1949; Reynolds and Brook, 1956; Larsen and Stansbury, 1974; Dye et al., 1989; Gremillion and Orville, 1999; Wolf, 2006]; however, the conditions associated with lightning cessation are relatively unknown. Improved knowledge about lightning cessation will be valuable since lightning is responsible for many deaths, injuries, and economic losses each year. Lightning is a particular concern for the daily operations of the NASA Kennedy Space Center (KSC) and Cape Canaveral Air Force Station (CCAFS) complex because many ground-based activities must be suspended until the threat has passed.

Forecasters at the 45th Weather Squadron (45WS) at KSC/CCAFS [Harms et al., 2003] issue lightning advisories when lightning poses a threat, and discontinue those advisories when the threat has passed [Weems et al., 2001; Bott and Eisenhower, 2005]. Although the 45WS is reasonably satisfied with their ability to forecast lightning initiation, they need improved guidance to determine when it is safe to cancel an advisory [Roeder, personal communication 2005; 2007]. In lieu of reliable forecast guidance for lightning cessation, the 45WS often leaves advisories in effect longer than later determined to be necessary, lest an advisory is ended too soon and safety is compromised. With over 25,000 employees, the monetary loss due to wasted manpower during lightning advisories is estimated to be millions of dollars each year [Roeder, personal communication 2005; 2007]. Increased knowledge about the behavior of dissipating storms over KSC/CCAFS will increase the 45WS's confidence that a particular

flash is the last flash of the storm, thus allowing a lightning advisory to be terminated sooner [Roeder and Glover, 2005].

Few studies have sought to understand lightning cessation. Hinson [1997] used radar data to identify a lag time of 30 min between the last 45 dBZ reflectivity at the -10°C level and the final cloud-to-ground (CG) strike. Holmes [2000] noted that each thunderstorm type (e.g., supercells, multicells, etc.) required a different regression model to forecast cessation. Roeder and Glover [2005] showed that a statistical approach to forecasting lightning cessation could yield promising results. The findings of Roeder and Glover [2005] motivated Stano et al. [2010] to use total lightning (i.e., intra-cloud [IC] and CG lightning) data to develop empirical lightning cessation forecast guidance for KSC. Stano et al. [2009] developed a dataset of 116 isolated thunderstorms from the warm seasons of 2000-2005 and identified correlations between lightning cessation and parameters from soundings and radar data. Although the maximum interflash time between any two flashes appeared to be a useful predictor for cessation, their results were far from ideal. It appeared that the probability of subsequent flashes was very low after 15 to 20 min without flash activity, but some outlier flashes could occur much later. The Stano et al. [2010] results provided the motivation for the current research.

Previous research also has suggested possible methods for predicting lightning cessation based on trends in storm characteristics during either lightning initiation or cessation. The onset of CG lightning has been related to values of radar-derived reflectivity at the heights of particular temperatures, such as the presence of 40 dBZ reflectivity at or above -10°C [e.g., Larsen and Stansbury, 1974; Dye et al., 1989; Gremillion and Orville, 1999; Wolf, 2006]. Wolf [2006] sought to forecast CG lightning initiation based on 40 dBZ reflectivity at or above -10°C altitude. He suggested that inverting the initiation criteria may be useful for

*Corresponding author address: Holly Melvin,
NOAA/NWS/MDL, 1325 East-West Highway,
Silver Spring, MD 20910,
email: Holly.Melvin@noaa.gov

forecasting cessation. Evaluating Wolf's suggestion is one of the goals of the current study.

This research builds on the few prior studies of lightning cessation by examining storm characteristics during the period leading up to cessation. We used Stano et al.'s [2010] dataset of 116 thunderstorms in the KSC/CCAFS area from May-September of 2000-2005 and employed data and recently developed tools from the Warning Decision Support System – Integrated Information (WDSS-II) software [Lakshmanan et al., 2007b] that were not available earlier. We consider the applicability of inverting lightning initiation criteria, such as Wolf [2006], to predict lightning cessation. This is achieved by analyzing reflectivity at the heights of specific temperatures (i.e., 0°C, -10°C, and -20°C) to investigate whether storms possess a common reflectivity value at these heights at the time of the last flash or, alternatively, if storms experience a common trend in values during the several minutes preceding cessation. Finally, storm characteristics such as changes in the heights of reflectivities are analyzed to gain additional insight into the behavior of storms in the minutes preceding cessation.

2. DATA AND METHODOLOGY

Three-dimensional VHF total lightning source data were provided by the Lightning Detection and Ranging (LDAR) network located at KSC/CCAFS [Lennon, 1975; Poehler and Lennon, 1979; Maier et al., 1995; Britt et al., 1998; Boccippio et al., 2001] (Figure 1, circles). We used a flash creation algorithm provided by the 45WS to group the LDAR-detected total lightning source emissions into flashes [Nelson, 2002]. Although LDAR was upgraded to the new LDAR-II system in April 2008 (Murphy et al., 2009), that is after our study period.

The KSC Cloud-to-Ground Lightning Surveillance System (CGLSS) [Roeder et al., 2005; Boyd et al., 2005] detects the ground strike locations of CG flashes (Figure 1, squares). CGLSS provides greater detection efficiency and location accuracy than the National Lightning Detection Network (NLDN) [Cummins et al., 1998; 1999; 2006] because of its shorter baseline [Roeder et al., 2000; Flinn et al., 2010] and is the preferred CG dataset for the KSC/CCAFS area [Boyd et al., 2005]; however, the CGLSS sensors are blinded by nearby

flashes with peak currents exceeding 40 kA [Ward et al., 2008]. To account for these unreported flashes, we used NLDN data to supplement the CGLSS data using a methodology provided by Roeder [personal communication, 2009] and based on Ward et al. [2008]. Details on this blending algorithm can be found in Anderson [2009]. In our 116 storm cases, NLDN flash data typically supplemented the CGLSS flash data by adding only one or two flashes per storm. CG flashes from the CGLSS/NLDN integrated database were linked to LDAR flashes using a flash matching algorithm [McNamara, 2002] to provide ground strike locations. CGLSS was upgraded to the CGLSS-II configuration in May 2008 [Murphy, 2008]; however, this is after our study period.

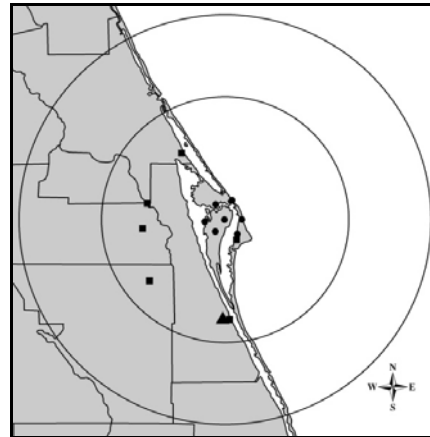


Figure 1. The research domain at KSC/CCAFS, where the outer ring (inner ring) is 100 km (60 km) from the central LDAR receiver. Locations of the sensors for the main observation networks are shown for LDAR (circles), CGLSS (squares), and the WSR-88D (triangle).

In addition to the lightning data, WSR-88D radar data from the NWS Forecast Office in Melbourne, FL (KMLB; Figure 1, triangle) were used to locate storms, visually assign flashes to storms, create radar-derived products, and derive storm characteristics. Whereas Stano et al. [2010] calculated storm environment parameters from morning radiosonde launches at Cape Canaveral, we used archived National Centers for Environmental Prediction (NCEP) Rapid Update Cycle (RUC) model analyses [Benjamin et al., 1994; 2004] to describe the storm environment near KSC. We used RUC40 (RUC20) hourly model analyses for the warm

seasons of 2000-2001 (2002-2005), following an increase in resolution during 2002.

The Warning Decision Support System – Integrated Information (WDSS-II; Lakshmanan et al., 2007b) software was used to define storm clusters, track the 116 storms selected by Stano et al. [2010], and obtain time-series of storm attributes from radar, RUC model analysis, and lightning parameters. The WSR-88D data from KMLB were quality-controlled [Lakshmanan et al., 2007a] and then interpolated onto a three-dimensional grid (0.01° latitude \times 0.01° longitude \times 1.0 km height, or about 1 km resolution) as data from each elevation angle of a volume scan were processed [Lakshmanan et al., 2006]. Radar products were produced approximately every 60 s, providing updated data at a shorter time interval than the typical 5-6 min volume scan.

The hierarchical K-Means storm clustering and tracking algorithm (i.e., w2segmotionll) within WDSS-II was used to identify and track storms through lightning cessation. Lakshmanan et al. [2003; 2009] and Lakshmanan and Smith [2009] provide detailed descriptions of the WDSS-II clustering algorithm. Briefly stated, since one must select the parameter that will be used to define the WDSS-II storm clusters, we tested several radar product-derived gridded fields with differing thresholds. Reflectivity fields were found to be spatially noisy, and the clustered storm area did not remain consistent as the gradient changed. Clusters based on VIL Density (i.e., VIL divided by the height of the 18 dBZ echo) [Amburn and Wolf, 1997] were the most consistent and most likely to track storms through lightning cessation. Pixels of VIL Density were located in the main convective core of storms (i.e., areas of strong dBZ), and our thresholds were tuned to cluster this core. Because VIL Density values were weak or nonexistent in a storm's anvil region, clusters did not include the anvil regions of storms. One hundred twenty statistics were calculated within each cluster at every time interval (approximately 60 s to 90 s), yielding time-series of parameters such as maximum composite reflectivity, average reflectivity at the -10°C altitude, and the maximum height of the 18 dBZ echo top. Because our clusters did not include a storm's anvil region, maximum values of cluster parameters are more reliable than area averages. Therefore, maximum values will be used in this study, as in previous studies [e.g., Zipser and Lutz, 1994; MacGorman et al.,

2007]. Maximum values of reflectivity and LDAR source density were obtained at 1 km intervals within each cluster to produce time-height displays.

Since our goal was to gather data prior to a storm's last flash, we did not require that WDSS-II track a storm from lightning initiation to cessation. Instead, we required that clustering begin at least two radar volume scans (~ 10 min) preceding the last flash and continue until the minute of the last flash. Each storm was carefully inspected to ensure that WDSS-II had clustered the storm's core consistently through the final flash and whether that flash occurred in the storm core or its anvil region. Not all of the original 116 storms could be included in the final dataset. Although many combinations of VIL Density thresholds were tested, we found it very difficult to consistently cluster and track weak, small, decaying storms through lightning cessation. As a result, our original dataset of 116 storms was reduced to 20 storms on 13 different days. Two of the 20 storms produced anvil lightning that was not considered in calculating the WDSS-II-derived parameters.

3. RESULTS

3.1 Case Study Examples

Time-height plots of total flash initiation sources and radar reflectivity are an important tool in this study since they show storm evolution over time. One should recall that WDSS-II cluster-derived statistics, such as reflectivity, LDAR source density, and 30 dBZ storm thickness, represent maximum values in the core of the storm, not the anvil region. Conversely, IC and CG flash initiation heights reflect all flashes occurring within the entire storm (including the anvil region). Therefore, this study relates maximum values of parameters within the core to lightning cessation in the entire storm. We do not account for charging within the anvil region or charge advection into the anvil region. One should recall that only two of the 20 storms produced anvil lightning. When analyzing the following time-height plots, one should note, for example, that a flash initiation height plotted in a region of 35 dBZ indicates that the flash initiated at the height where the maximum reflectivity is 35 dBZ within the core. It does not necessarily indicate that the flash initiated in a region of 35 dBZ. Our investigation into the behavior of decaying cells

using WDSS-II cluster-derived data begins by presenting two examples of how storms behave during decay.

Case 1 - Single Cell on 17 May 2002

Figure 2 is the time-height plot of several parameters for a typical single cell on 17 May 2002. The WDSS-II cluster-derived radar and LDAR source density data encompass the duration of lightning activity, from before the first flash at 1940:47 UTC until after the last flash at 2044:57 UTC. Greatest source densities occur at ~1956 UTC, ~33% through the storm's duration. Thus, greatest source densities in the storm's core occur near the middle of its life cycle when reflectivities greater than 40 dBZ extend higher than 7 km (the height of the -10°C isotherm). Most IC flashes initiate above the freezing level (0°C). The few that do not probably represent data uncertainty. CG flashes generally originate below the height of the -10°C isotherm. The reflectivity contours remain at a relatively constant height during most of the storm's lifetime, but descend during the last several minutes. The 40 dBZ echo descends below the height of -10°C by the time of the last lightning flash, an IC flash at 2044:57 UTC.

Case 2 - Single Cell on 13 August 2000

Figure 3 illustrates a single cell storm that occurred on 13 August 2000. WDSS-II cluster statistics begin ~2 min after lightning initiation. One should note the absence of lightning activity between 2049 and 2107 UTC. While no lightning occurs during this 18 min period, a final IC flash does occur at 2107:29 UTC. This is one of the 6 storms in the original 116 storm dataset that experiences an "outlier"-type of decay [Stano et al., 2010], with an apparent cessation at ~2047 UTC and one last "surprise" IC flash at 2107:29 UTC. IC flash initiations again are located above the 0°C isotherm (Figure 3); however, a comparison of reflectivity profiles (Figures 2 and 3) shows that the altitudes of flash initiations and source density contours are

more dispersed in the current storm (Figure 3). The greatest source density again occurs at ~2027 UTC, about 33% through the storm's duration. One should note that the height of -20°C is 9 km (1 km higher than in the previous case). Contours of reflectivity exceeding 35 dBZ are at a nearly constant altitude below -10°C throughout the last 40% of the storm duration, from ~2046 to 2107 UTC, with downward sloping occurring only after the last flash. There is no clear indication that this storm will experience an "outlier" cessation behavior; however, reflectivity contours near the end of its lifecycle are more constant in altitude than the other two cases in this section. We hypothesize that the nearly constant reflectivity contours below -10°C indicate a small rate of electrification. Charge may build up gradually in the storm until the breakdown threshold is finally reached, resulting in the final IC flash.

3.2 Storm Characteristics during the Minutes Leading to Lightning Cessation

While time-height plots of individual storm cells are of great interest, histogram plots (e.g., Figure 4) describe the overall trends in reflectivity characteristics for all 20 storms as a group. Histogram plots in this study focus on the 8 min before the last flash. The 8 min threshold focuses on the end of lightning activity and is the first time prior to cessation that WDSS-II cluster-derived data are available for all 20 storms.

Alternatively, composite plots (e.g., Figure 5) allow us to examine changes in the mean, range, and standard deviation of storm parameters at 1 min intervals prior to lightning cessation. For a parameter to indicate imminent cessation, it should exhibit a decreasing mean as well as a convergence of values. The decreasing mean suggests that the storm parameter is related to cell decay. The convergence of values and decreasing standard deviation might indicate a threshold at which cessation is expected.

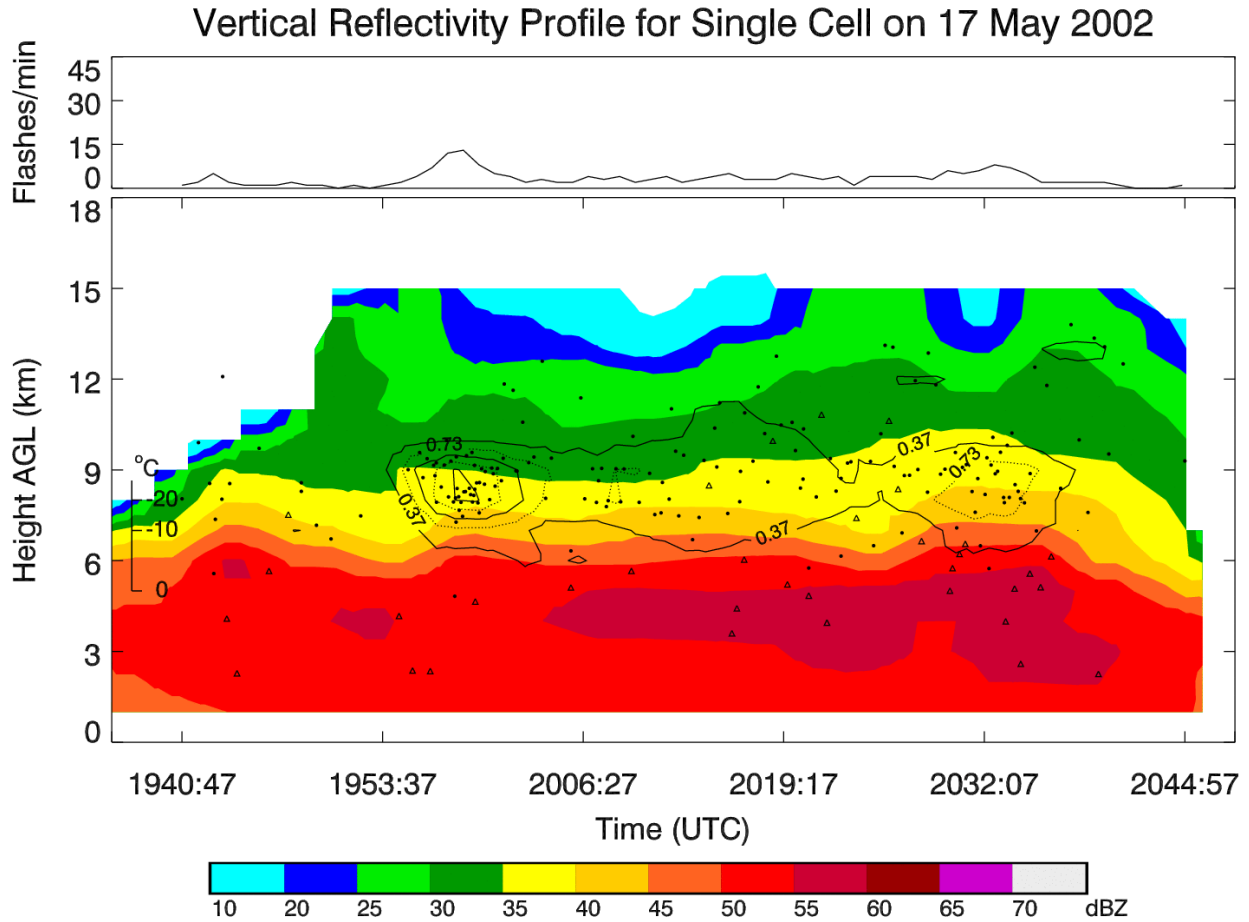


Figure 2. Time-series of the vertical profile of cluster-derived maximum reflectivity (color shaded, dBZ), cluster-derived maximum LDAR source density (black contours, sources $\text{min}^{-1} \text{km}^{-2}$), IC and CG lightning flash initiation sources (circles and triangles, respectively) within the entire storm (anvil region included), for a single cell storm on 17 May 2002. To preserve readability, the LDAR source density contour for 0 sources $\text{min}^{-1} \text{km}^{-2}$ has not been plotted. Similar to previous figures, data are time-normalized; the first (last) time that is noted (UTC) corresponds to the first (last) flash of the storm. The resolution of both the cluster-derived radar data and cluster-derived LDAR source density is 1 km at a 60-90 s time resolution, whereas flash initiation heights are taken from the raw data. Cluster-derived maximum heights of the environmental 0°C , -10°C , and -20°C isotherm levels within the cluster are plotted as bars on the left side of the figure. The upper plot is total lightning flash rate per min.

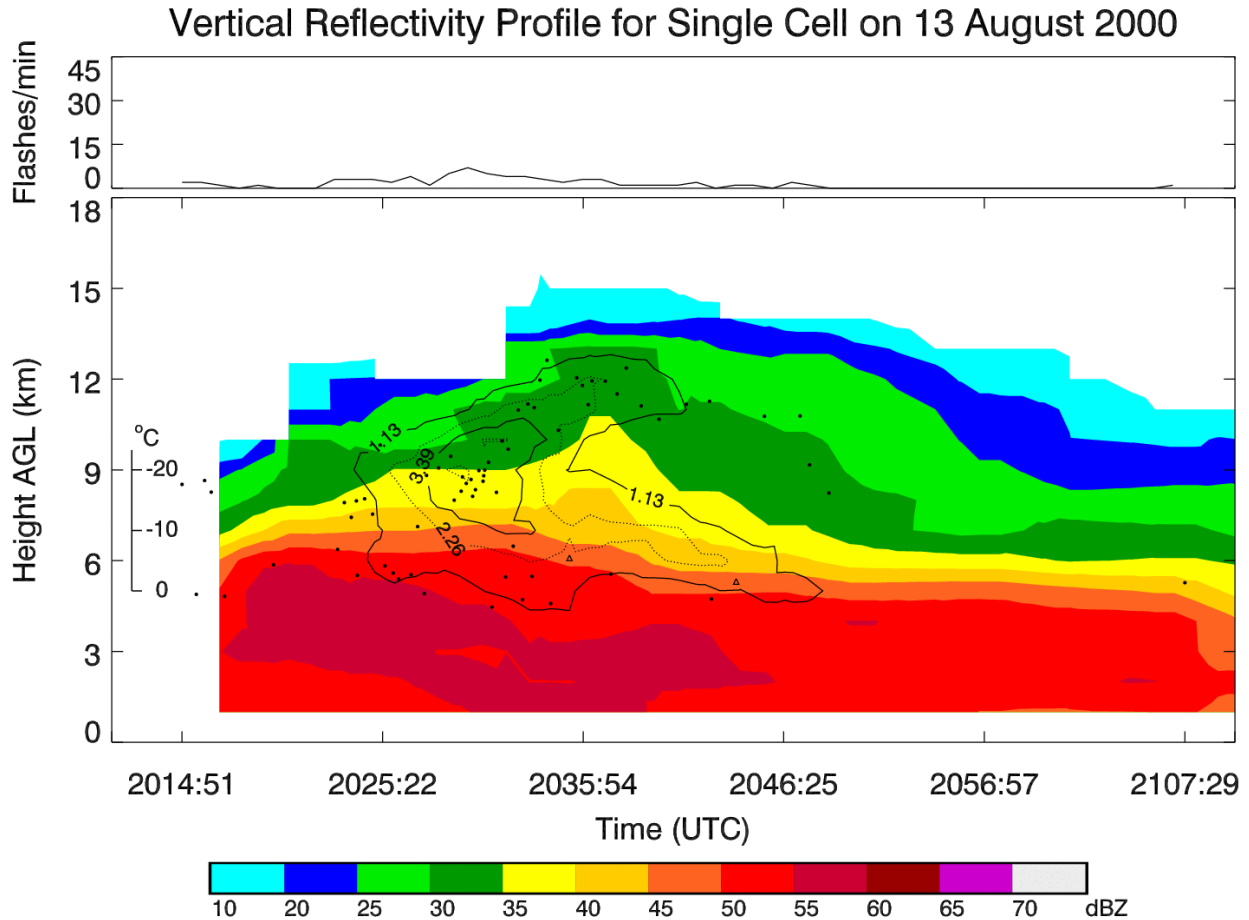


Figure 3. As in Figure 2, except for a single cell storm on 13 August 2000.

3.2.1 *Composite Reflectivity*

The distribution of 8 min trends in maximum composite reflectivity is shown in Figure 4. Values were calculated by subtracting the value 8 min prior to cessation from the value at cessation. The values are divided into 10 equal bins. Positive (negative) values indicate that the reflectivity was increasing (decreasing) during the 8 min prior to cessation. Sixteen of the 20 storms (80%) exhibit decreasing reflectivity whereas the reflectivity of 4 storms increases. The distribution does not indicate a typical magnitude of change during the 8 min prior to cessation. The fact that composite reflectivities in some storms slightly increases suggests that storms decay at different rates and may even intensify slightly prior to the last flash, even though a general trend of decay occurs during the latter part of a storm's duration.

The plot of maximum composite reflectivity (Figure 5) shows the mean decreasing only 3 dBZ during the 8 min period prior to cessation, from 53.5 dBZ to 50.5 dBZ; however, the standard deviation increases ~1.4 dBZ. Thus, there is no major change in the mean or range during the 8 min prior to cessation, and because the standard deviation increases, composite reflectivity varies more at cessation than during the preceding minutes. This is reasonable since storms of varying intensity probably decay at different rates (Figure 4). However, the small decrease and increasing standard deviation indicate that this parameter is not useful for predicting cessation.

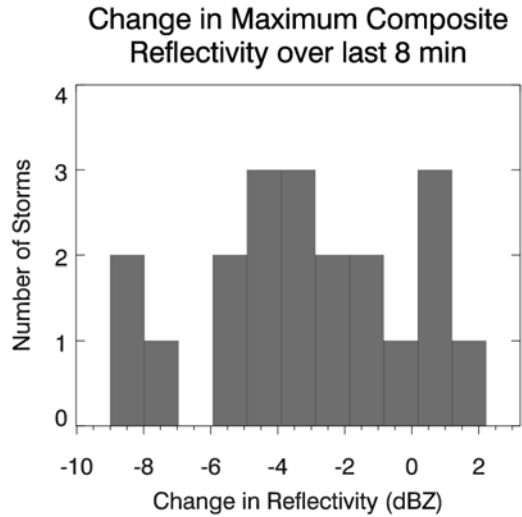


Figure 4. Distribution of trends in maximum composite reflectivity within each cluster during the 8 min prior to cessation. Values were calculated by subtracting the value 8 min prior to cessation from the value at cessation. The values are divided into 10 equal bins. Positive (negative) values indicate that the reflectivity was increasing (decreasing) during the 8 min prior to cessation.

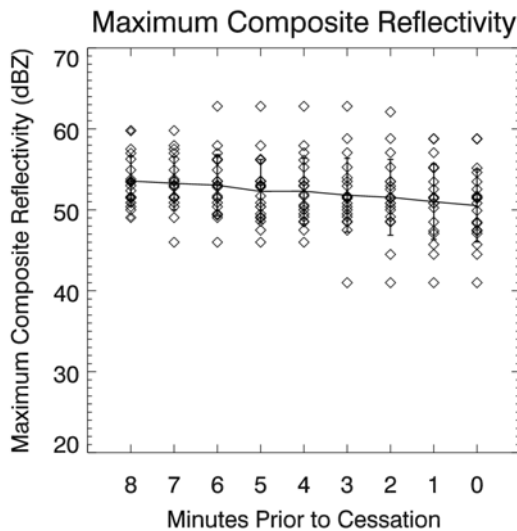


Figure 5. Time trend of the mean (thick black line) and standard deviation (vertical lines) of maximum composite reflectivity (dBZ) at 1 min intervals beginning 8 min prior to the last flash, $t = 0$. Values for the 20 storm cases are superimposed at 1 min intervals (diamonds).

3.2.2 Radar Reflectivity at Various Temperatures

Several studies have suggested that cessation can be estimated by inverting lightning initiation criteria. However, this has yet to be proven. While continued electrification may have subsided and the previously generated electric charge should slowly dissipate, the hydrometeors can carry the previously generated electric charge for large periods of time. As centers of charge move about in the decaying storm, they may come closer to other charge centers of opposite sign and produce another lightning flash. This may be a source for some of the long delayed “outlier” flashes discussed earlier. The most common criterion to predict initiation is the presence of 40 dBZ reflectivity at or above -10°C [e.g., Gremillion and Orville, 1999; Vincent et al., 2003; Wolf, 2006]. Hinson [1997] found that descent of the 45 dBZ echo below -10°C preceded CG cessation by approximately 30 min in three storms at KSC. However, both Wolf [2006] and Hinson [1997] only focused on predicting CG lightning; IC flashes were not considered. Our study differs in that LDAR-derived total lightning data allow us to investigate the applicability of applying these radar criteria to the cessation of total lightning.

Wolf [2006] forecast the onset and frequency of lightning using the height of 40 dBZ reflectivity above -10°C , noting that a higher echo indicates a greater amount of hydrometeors in the updraft and therefore an increased probability of lightning. Current WDSS-II tools did not allow us to gather direct statistics on the height of the 40 dBZ echo above -10°C ; however, other statistics were available to approximate this relationship near the storm’s core. These parameters are maximum reflectivity at the environmental 0°C , -10°C , and -20°C levels within each cluster.

We begin by investigating trends in reflectivity at these temperatures and the average reflectivity in the 0°C to -20°C layer during the 8 min prior to cessation. We expected that reflectivities would decrease in decaying cells, since reflectivity cores descend to the surface during the storm dissipation stage [Byers and Braham, 1949]. Figures 6 a-c show that 18 of our 20 storms (90%) do exhibit decreasing reflectivity at the three temperatures during the 8 min preceding cessation. However,

each distribution also shows two cases of increasing reflectivity. The first is attributed to a storm that exhibits slightly increasing reflectivity at all three levels. This increase is a result of the time period chosen, since there is a clear overall trend of decay, with reflectivities decreasing from their peak at ~30% through

storm duration. The second case of increasing reflectivity at each level can be attributed to three separate storms that increase at one level, but decrease at the other two. This indicates that reflectivities do not descend uniformly during decay.

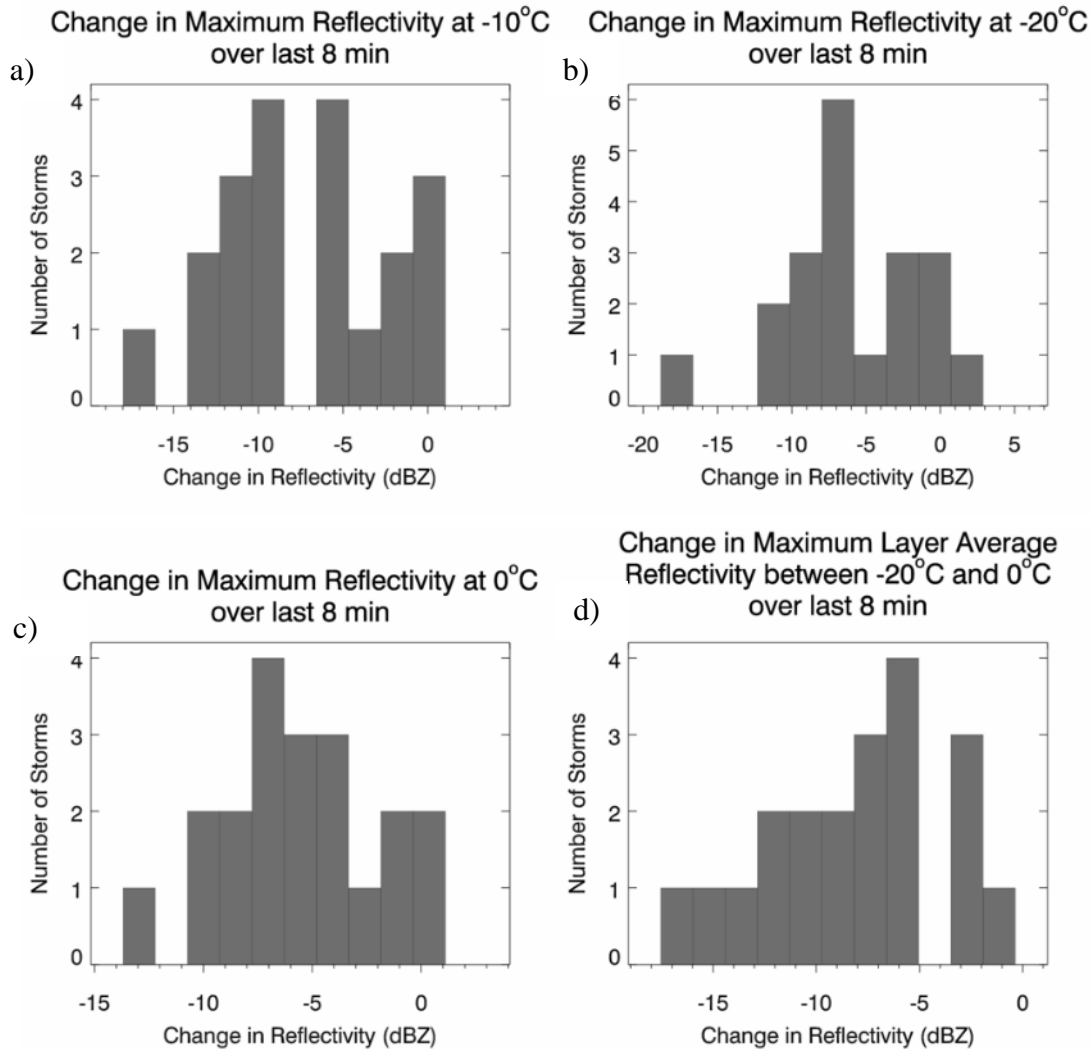


Figure 6. As in Figure 4, except for a) maximum reflectivity at -10°C , b) maximum reflectivity at -20°C , c) maximum reflectivity at 0°C , and d) maximum layer-averaged reflectivity between 0°C and -20°C .

Since the mixed phase region between 0°C and -20°C is vital to storm electrification [e.g., Takahashi, 1978; Jayaratne et al., 1983; Saunders et al., 1991], layer-averaged reflectivity between these temperatures should indicate the amount of hydrometeors in the region and therefore serve as a proxy for the

amount of charging and lightning that is occurring [e.g., Dye et al., 1986]. We expected decaying storms to exhibit decreasing layer-averaged reflectivity as the reflectivity cores descend. Results show that maximum layer-averaged reflectivity between 0°C and -20°C (Figure 6d) is the only parameter that decreases

in all 20 storms. However, the distribution is skewed to the left, indicating that the reflectivities typically decrease less than ~7 dBZ during the 8 min period prior to cessation. This small value does not suggest operational utility in forecasting cessation.

To investigate further, plots of actual reflectivity at 0°C, -10°C, -20°C, and layer-averaged reflectivity between 0°C and -20°C for all 20 storms are shown at 1 min intervals in Figure 7. Results indicate that reflectivities decrease at all three temperatures and in the layer average. Considering the -10°C level first (Figure 7a), one should note that although 40 dBZ reflectivity does not always descend below -10°C prior to cessation, values at the last flash do cluster around 40 dBZ. In addition, the mean decreases from 45.9 dBZ to 38.6 dBZ during the 8 min prior to cessation. Although the average decreases, Figure 6 showed that two storms exhibit increased reflectivity at -10°C prior to cessation. The standard deviation of reflectivity at -10°C also decreases 1.72 dBZ during this 8 min time period, indicating that variability decreases as cessation approaches. Moving higher, reflectivity at -20°C (Figure 7b) decreases from 39.5 dBZ 8 min before cessation to 33.6 dBZ at the last flash. The range decreases, and the standard deviation decreases by 1.55 dBZ. Finally, reflectivity at 0°C (Figure 7c) decreases from 53.6 dBZ to 46.7 dBZ. Although the standard deviation of reflectivities at 0°C is smaller than at the other two temperatures prior to cessation, it actually increases 2 dBZ as cessation approaches. In fact, reflectivity at 0°C is the only parameter whose standard deviation increases as cessation approaches. The range of values is between 59.8 dBZ and 46.1 dBZ 8 min before cessation, increasing to between 58.8 dBZ and 34.3 dBZ at cessation. This indicates more variability at the time of cessation than 8 min earlier and that reflectivity at 0°C may not be the best temperature to use when predicting cessation.

Average reflectivity in the mixed layer between 0°C and -20°C (Figure 7d) decreases the most during the 8 min period, 8.3 dBZ. Its standard deviation remains nearly constant, 6.4 dBZ (6.3 dBZ) 8 min prior (at) cessation. Although this decrease is the greatest of all four parameters, the lack of convergence to a particular value indicates that this parameter will not be useful to predict cessation.

To summarize, reflectivity at -10°C appears to be the best indicator of cessation. Although its mean does not decrease as much as layer-averaged reflectivity, it does decrease more than at 0°C and -20°C and the decrease in standard deviation indicates less variability at the time of cessation than 8 min before. Conversely, reflectivity at 0°C is the least useful for predicting cessation since there is more variability at the last flash than earlier.

3.2.3 30 dBZ Vertical Storm Thickness above -10°C

The maximum height of 30 dBZ above -10°C is another WDSS-II parameter that provides information about a storm's decay. It can be interpreted as a measure of the vertical thickness of the 30 dBZ echo [MacGorman et al., 2007]. A lower 30 dBZ echo above -10°C indicates a smaller mass of precipitation within the mixed phase region, and therefore a smaller probability of lightning production [Vincent et al., 2003]. The parameter decreases in 15 cells (75%) during the 8 min leading to cessation (Figure 8). However, five cells (25%) exhibit an increase in thickness.

The composite plot of maximum height for the remaining storms (Figure 9) shows that the mean decreases ~3.2 km during the 8 min period. It is important to note, however, that the 30 dBZ echo oscillates around -10°C within one storm during the period, and descends below -10°C in a second; data were unavailable for these storms during the minutes when 30 dBZ was located below -10°C. Thus, these storms were not included in calculating the mean and standard deviation of this parameter during those times. Eight minutes before cessation, values range from 6.73 km to 0.10 km. By the last flash, the 30 dBZ echo in one storm reaches 3.72 km above -10°C, but in another it descends below the -10°C level. Standard deviations decrease from 1.81 km to 1.01 km cessation.

Although the height of 30 dBZ does increase in five storms prior to cessation (Figure 8), the decreases in mean and standard deviation support the hypothesis that a lower 30 dBZ above -10°C likely indicates a smaller probability of lightning [Vincent et al., 2003]. The oscillations in 30 dBZ reveal that 30 dBZ does not descend uniformly during the 8 min prior to cessation. Nevertheless, the large range of values at cessation indicates that it will not be a useful forecasting parameter.

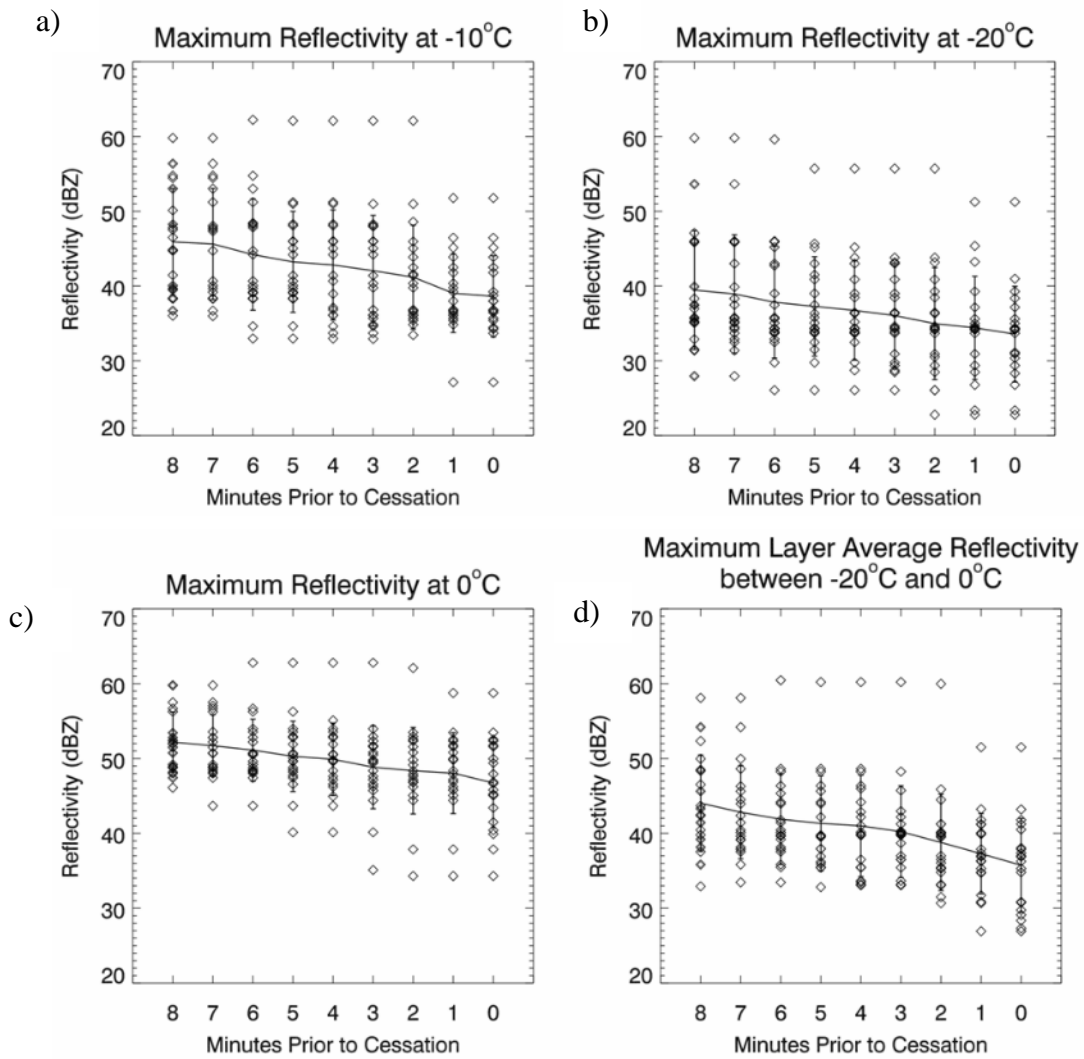


Figure 7. As in Figure 5, except for a) maximum reflectivity at -10°C (dBZ), b) maximum reflectivity at -20°C (dBZ), c) maximum reflectivity at 0°C (dBZ), and d) maximum layer-averaged reflectivity between 0°C and -20°C (dBZ).

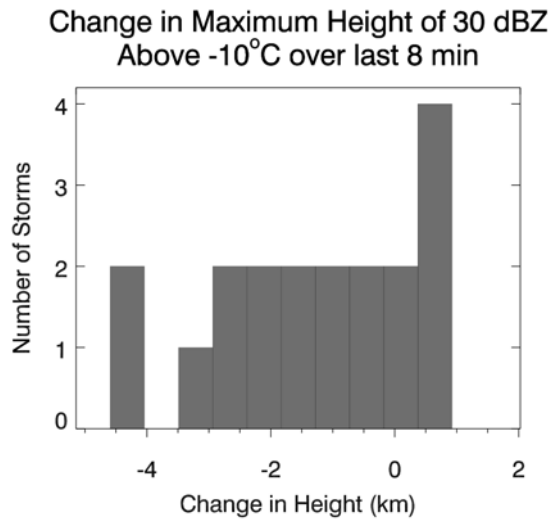


Figure 8. As in Figure 4, except for maximum height of the 30 dBZ radar reflectivity echo above the -10°C level (i.e., vertical 30 dBZ storm cell thickness). The histogram consists of only 19 storms since one storm did not have a 30 dBZ echo above the -10°C level at the last flash and therefore a trend could not be computed.

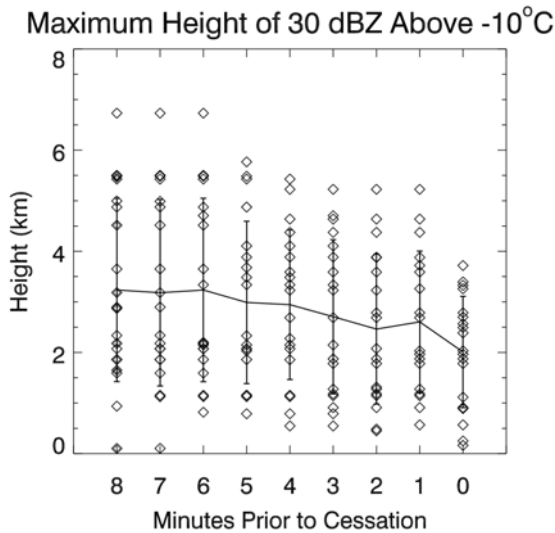


Figure 9. As in Figure 5, except for maximum height of the 30 dBZ radar reflectivity echo above the -10°C level (i.e., vertical 30 dBZ storm cell thickness).

3.3 Storm Characteristics at the Time of Lightning Cessation

We began by examining trends in various storm characteristics during the 8 min period prior to cessation. The goal was to determine whether there were trends during the end of the storm lifecycle. Although trends were evident in some parameters, none appeared to be a reliable indicator of imminent lightning cessation. Therefore, we next examine distributions of these characteristics at the time of the last flash to determine if there is a preferred value at lightning cessation. If this is the case, a decaying cell's convergence to this value might be a signal of impending lightning cessation. We also continue to consider the applicability of inverting lightning initiation criteria to predict lightning cessation.

3.3.1 Composite Reflectivity

Maximum composite reflectivity for the majority of the 20 storms was found to decrease during the 8 min prior to the last flash (Figure 4). Figure 10 shows that some storms have maximum last flash composite reflectivities as small as ~ 41 dBZ and as large as ~ 58 dBZ, with the distribution peaking in the middle of the range. The majority of storms (15 of 20; 75%) have composite reflectivities between ~ 46 dBZ to ~ 55 dBZ. Thus, storms do cluster within a relatively small range of values at the last flash. However, one should note that composite reflectivities still exceed ~ 40 dBZ at the time of the last flash, indicating the cell's intensity is still moderate to strong.

3.3.2 Radar Reflectivity at Various Temperatures

We next determine if most storms exhibit a specific reflectivity at one of the three temperatures (i.e., 0°C , -10°C , and -20°C) at the time of cessation. Thus, we continue to determine the applicability of inverting lightning initiation criteria for predicting cessation. One should recall that the most common criteria to predict lightning initiation is the presence of 40 dBZ reflectivity at -10°C [e.g., Gremillion and Orville, 1999; Vincent et al., 2003; Wolf, 2006]. Current results show that 14 of the 20 cells (70%) have a reflectivity less than 40 dBZ at -10°C at cessation, indicating that the 40 dBZ echo has descended below this value prior to

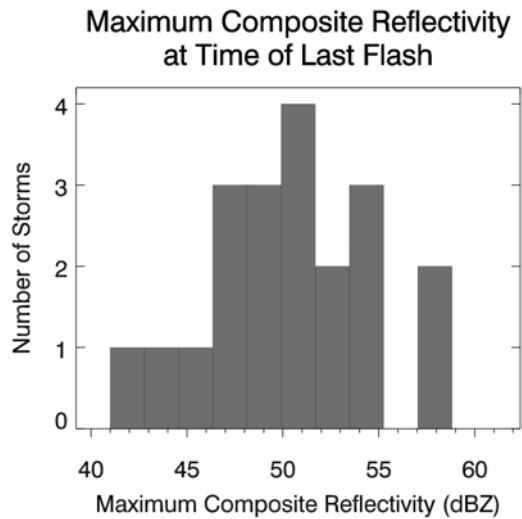


Figure 10. Distribution of maximum composite reflectivity (dBZ) at the last flash for the 20 storms. The values are divided into 10 equal bins.

cessation. However, 6 cells (30%) exceed 40 dBZ at -10°C (Figure 11a), and 3 cells exhibit reflectivity greater than 45 dBZ at the last flash. In fact, the reflectivity of one cell at -10°C exceeds 50 dBZ at cessation. Therefore, the cessation criteria of descent of 45 dBZ below the -10°C level noted by Hinson [2002] would not provide good guidance for our storm population.

Figure 11b shows that 18 cells (90%) exhibit reflectivities less than 40 dBZ at the -20°C level; however, the distribution shows even less indication of a threshold than at -10°C . Maximum reflectivity at 0°C (Figure 11c) exhibits a similar pattern. Figure 11d shows the distribution of maximum layer-averaged reflectivity between -10°C and -20°C . Although all cells exhibit values greater than 25 dBZ at the last flash, the distribution, ranging from 26.9 to 51.5 dBZ, does not suggest that storms converge to a typical value. When all four distributions are compared, the distribution of reflectivity at -10°C most supports the existence of a preferred value, since 13 storms have last flash values between 32.1 and 39.5 dBZ. This suggests that even though the presence of 40

dBZ at -10°C may not be the most accurate criteria for forecasting cessation, the greatest possibility of discovering applicable lightning cessation criteria may lie in some reflectivity value at that temperature.

To summarize, reflectivities at -10°C indicate that a simple inversion of the Wolf [2006] and Hinson [2002] criteria would be unsuitable for predicting cessation in our storm dataset. It does not appear that storms exhibit a preferred reflectivity at the 0°C , -10°C , or -20°C levels, or in average reflectivity between 0°C and -20°C . The ranges of reflectivities are too large to suggest a threshold that could help determine imminent cessation.

3.3.3 30 dBZ Vertical Storm Thickness above -10°C

The distribution of maximum heights of 30 dBZ reflectivity above -10°C (Figure 12) shows that 30 dBZ does not extend more than 3.72 km above -10°C at the last flash. In fact, one storm's 30 dBZ echo descends below -10°C prior to the last flash. Several bins have the same number of storms, and no preferential value is evident. Storms do not possess a certain value at the last flash.

4. SUMMARY AND CONCLUSIONS

Trends in composite reflectivity, reflectivity at three temperatures crucial to storm electrification (i.e., 0°C , -10°C , -20°C) and storm thickness of 30 dBZ above -10°C were analyzed for 20 storms during the 8 min period prior to cessation to determine if any indicated imminent cessation. Results showed substantial variability in the decaying storms. Although these parameters decreased in most storms during the 8 min period, some increased. Distributions of the parameters at the last flash also were considered, but no clearly preferred value was evident at the last flash. Neither the inversion of lightning initiation criteria (e.g., 40 dBZ at -10°C) nor the descent of 45 dBZ below -10°C were found to be a useful indicator of cessation.

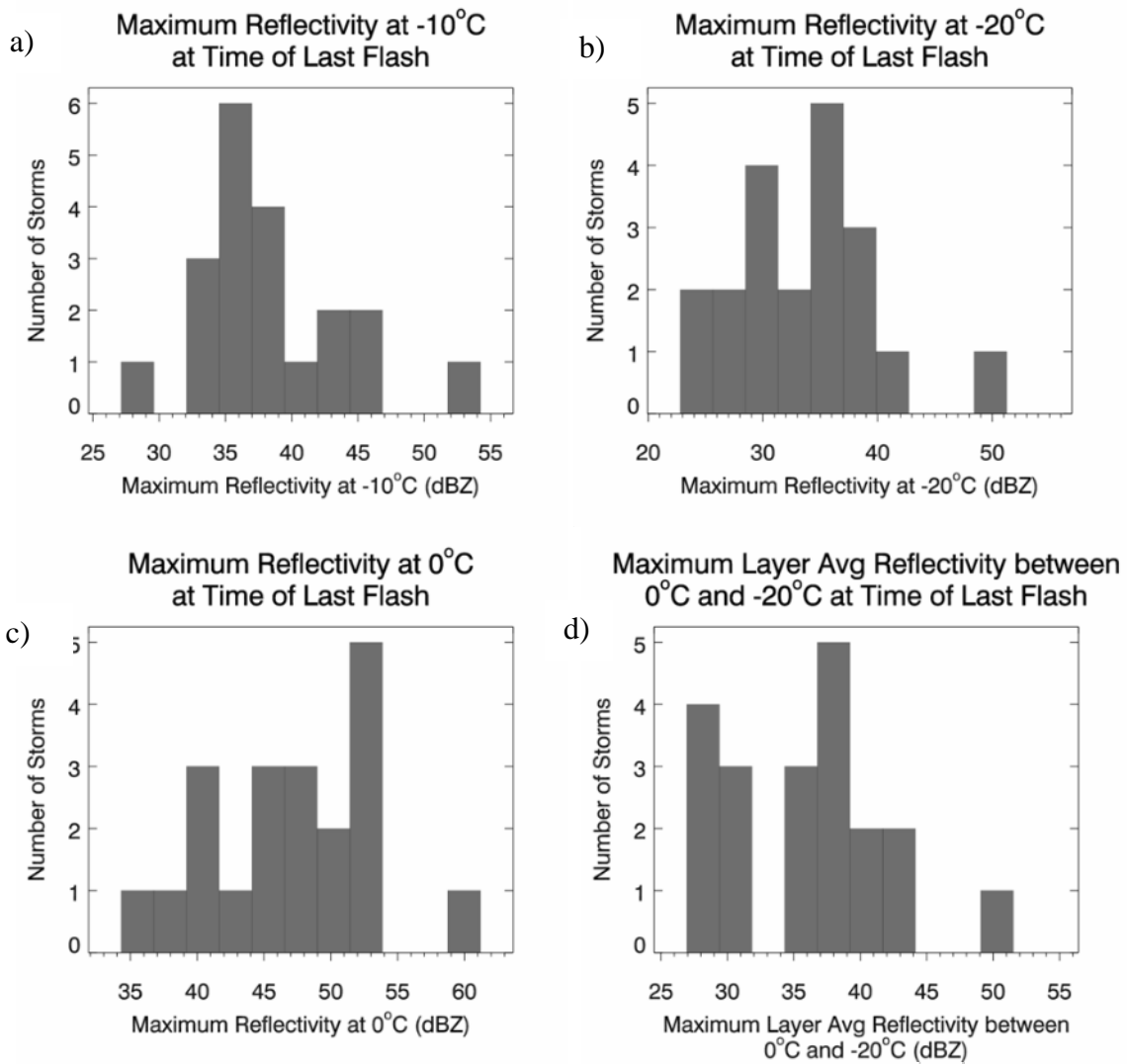


Figure 11. As in Figure 10, except for a) maximum reflectivity (dBZ) at the -10°C level, b) maximum reflectivity (dBZ) at the -20°C level, c) maximum reflectivity (dBZ) at the 0°C level and d) maximum layer-averaged reflectivity (dBZ) between 0°C and -20°C .

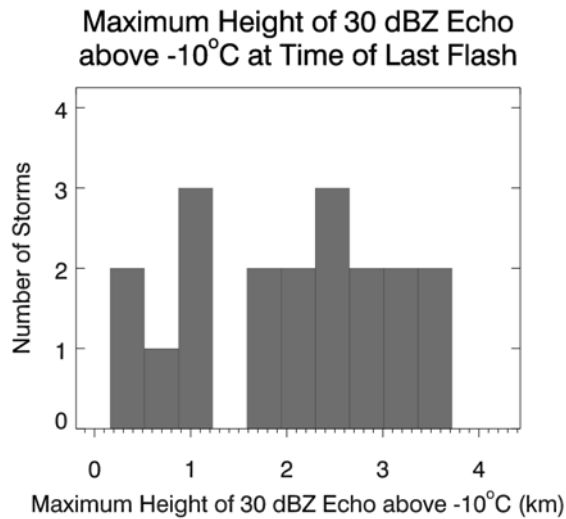


Figure 12. As in Figure 10, except for the maximum height of the 30 dBZ echo above the -10°C level at the last flash. The histogram consists of only 19 storms since one storm did not have a 30 dBZ echo above the -10°C level at the last flash.

Various characteristics of 20 WDSS-II-tracked storms also were studied, searching for a parameter that would decrease quickly and converge to a specific value during the 8 min prior to lightning cessation. Composite reflectivity decreased for the majority of storms prior to cessation, but it increased for a few storms (Figure 4). Although mean composite reflectivity decreased slightly (Figure 5), its standard deviation increased, indicating that composite reflectivity varied more at cessation than 8 min earlier. The increasing standard deviation indicates that this parameter would not be useful for predicting cessation. Reflectivities at three temperatures (0°C , -10°C , and -20°C) and layer-averaged reflectivity between 0°C and -20°C (Figures 6 and 7) also were examined prior to the last flash. Although our data did not indicate a preferred reflectivity value at 8 min prior to cessation or at the last flash (Figures 10 – 12), the -10°C temperature exhibited the greatest potential for indicating lightning cessation. The 0°C temperature was the least reliable value for predicting cessation. Although layer-averaged reflectivity between 0°C and -20°C exhibited the greatest decrease between cessation and 8 min prior to cessation, its

variability did not converge prior to cessation. Thus, it would not be a good indicator of cessation. This indicates that dissipating storms decay at different rates and that radar reflectivities do not descend uniformly during cessation.

The vertical thickness of 30 dBZ reflectivity above -10°C decreased in the majority of storms during the 8 min prior to cessation (Figure 9 and 12). All 20 storms were within 3.72 km above or had descended below -10°C at the last flash. The 30 dBZ echo oscillated around the -10°C level prior to cessation in one storm, indicating that reflectivities do not always descend uniformly during dissipation, but may increase and decrease.

Our study was motivated by the 45WS' need for improved guidance to determine when it is safe to terminate lightning advisories at KSC/CCAFS. However, the current results reveal the inherent difficulty in forecasting cessation since storm characteristics exhibit considerable variability during decay and at the time of the last flash. For example, the 20 isolated storms displayed composite reflectivities between ~ 41 to ~ 58 dBZ at cessation. Reflectivities at -10°C may be as small as ~ 27 dBZ, but can exceed 50 dBZ. The height of 30 dBZ can be as high as 3.72 km above -10°C , but may be below this level at cessation. Eight-minute trends prior to cessation show that reflectivity parameters can increase or decrease in the 8 min prior to cessation. In summary, no definitive technique to reliably forecast lightning cessation was feasible.

In order to increase the statistical confidence that safe operational guidelines can be established, a larger dataset must be developed. Cool season (October-April) storms also should be considered. The processes leading to anvil lightning (i.e., charging within the anvil region or charge advection into the anvil) should be investigated since they may differ from processes that produce lightning in the storm core.

The current results indicate that much remains to be learned about lightning cessation. Future research must consider the evolution of hydrometeor configurations during storm duration. This will require polarimetric radar data that recently became available at KSC and will become available nationwide as the current WSR-88D radars are modified. The strength of polarimetric radar is its capability to identify hydrometeor types (e.g., hail, graupel, ice,

snow) that are crucial to electrification [e.g., Höller et al., 1994; Vivekanandan et al., 1999]. We expect that relating hydrometeor configurations with the locations of charge regions during the storm lifecycle, particularly during the dissipation phase, will yield valuable insights into storm dissipation and how lightning cessation can be forecast.

5. ACKNOWLEDGEMENTS

Special thanks go to Bill Roeder of the 45th Weather Squadron for his help and insight on this research. This research was sponsored in part by a 2007-2008 American Meteorological Society Graduate Fellowship sponsored by Lockheed Martin Corporation. Additional funding was provided by a grant from the NASA Florida Space Grant Consortium.

6. REFERENCES

- Amburn, A. A., and P. L. Wolf (1997), VIL density as a hail indicator, *Wea. Forecasting*, 12, 473–478.
- Anderson, Holly A. (2009), Characteristics of Decaying Storms During Lightning Cessation at Kennedy Space Center and Cape Canaveral Air Force Station, M.S. Thesis, Dec 2009, The Florida State University, 75 pp.
- Benjamin S. G., K. J. Brundage, P. A. Miller, T. L. Smith, G. A. Grell, D. Kim, J. M. Brown, and T. W. Schlatter (1994), The Rapid Update Cycle at NMC. Preprints, 10th Conf. on Numerical Weather Prediction, Portland, OR, Amer. Meteor. Soc., 566–568.
- Benjamin, S.G., D. Dévényi, S.S. Weygandt, K.J. Brundage, J.M. Brown, G.A. Grell, D. Kim, B.E. Schwartz, T.G. Smirnova, T.L. Smith, and G.S. Manikin (2004), An Hourly Assimilation–Forecast Cycle: The RUC. *Mon. Wea. Rev.*, 132, 495–518.
- Boccippio, D. J., S. J. Heckman, and S. J. Goodman (2001), A diagnostic analysis of the Kennedy Space Center LDAR network. 1. Data characteristics. *J. Geophys. Res.*, 106, 4769–4786.
- Bott, T. F., and S. W. Eisenhauer (2005), Development of optimal lightning warning procedures using probabilistic risk analysis. Conference on Meteorological Applications of Lightning Data, 9-13 Jan 05, 11 pp.
- Boyd, B. F., W. P. Roeder, D. L. Hajek, and M. B. Wilson (2005), Installation, upgrade, and use of a short baseline cloud-to-ground lightning surveillance system in support of space launch operations, Conference on Meteorological Applications of Lightning Data, 9-13 Jan 05, 4 pp.
- Britt, T. O., C. L. Lennon, and L. M. Maier (1998), Lightning Detection and Ranging System. NASA Tech Brief, Vol. 22, Issue 4, 60-61.
- Byers, H. R., and R. R. Braham (1949), The Thunderstorm. Supt. of Documents, U.S. Government Printing Office, Washington D.C., 287 pp.
- Cummins, K. L., M. J. Murphy, E. A. Bardo, W. L. Hiscox, R. B. Pyle, and A. E. Pifer (1998), A combined TOA/MDF technology upgrade of the U.S. National Lightning Detection Network, *Journal of Geophysical Research*, 103, 9035-9044.
- _____, R. B. Pyle, and G. Fournier (1999), An integrated American lightning detection network, 11th International Conference on Atmospheric Electricity, 7-11 Jun 99, 218-221.
- _____, K. L., J. A. Cramer, C. J. Biagi, E. P. Krider, J. Jerauld, M. A. Uman, V. A. Rakov (2006), The U.S. National Lightning Detection Network: Post-upgrade status, 2nd Conf. on Meteorological Appl. of Lightning Data, AMS Annual Meeting, Atlanta, 2006.
- Dye, J. E., W. P. Winn, J. J. Jones, and D. W. Breed (1989), The electrification of New Mexico thunderstorms. Part I: Relationship between precipitation development and the onset of electrification. *J. Geophys. Res.*, 94, 8643–8656.
- Flinn, F. C., W. P. Roeder, D. J. Pinter, S. M. Holmquist, M. D. Buchanan, T. M. McNamara, M. McAleenan, K. A. Winters, P. S. Gemmer, M. E. Fitzpatrick, and R. D. Gonzalez, 2010: Recent improvements in lightning reporting at 45th Weather Squadron, 14th Conference on Aviation, Range, and Aerospace Meteorology, Paper 7.3, 17-21 Jan 2010, 14 pp.
- Gremillion, M. S., and R. E. Orville (1999), Thunderstorm characteristics of cloud-to-ground lightning at the Kennedy Space Center, Florida: A study of lightning initiation signatures as indicated by the WSR-88D. *Wea. Forecasting*, 12, 640-649.

- Harms, D. E., B. F. Boyd, F. C. Flinn, J. T. Madura, T. L. Wilfong, and P. R. Conant (2003), Weather systems upgrades to support space launch at the Eastern Range and the Kennedy Space Center, 12th Symposium on Meteorological Observations and Instrumentation, 9-13 Feb 03, Long Beach, CA, Paper 7.1, 9 pp.
- Hinson, M. S. (1997), A study of the characteristics of thunderstorm cessation at the NASA Kennedy Space Center, M.S. Thesis, Aug 1997, Texas A&M University, 91 pp.
- Höller, H., Bringi, V.N., Hubbert, J., Hagen, M. and Meischner, P.F. (1994), Life cycle and precipitation formation in a hybrid type hailstorm revealed by polarimetric and Doppler radar measurements. *J. Atmos. Sci.*, 51, 2500-22.
- Holmes, M. W. (2000), Techniques for forecasting the cessation of lightning at Cape Canaveral Air Station and the Kennedy Space Center, M.S. Thesis, Air Force Institute of Technology, 90 pp.
- Lakshmanan, V., R. Rabin, and V. DeBrunner (2003), Multiscale Storm Identification and forecast. *J. Atm. Res.*, 67, 367-380.
- Lakshmanan, V., T. Smith, K. Hondl, G. J. Stumpf, and A. Witt (2006), A real-time, three dimensional, rapidly updating, heterogeneous radar merger technique for reflectivity, velocity and derived products. *Wea. Forecasting*, 21, 802–823.
- Lakshmanan, V., A. Fritz, T. Smith, K. Hondl, and G. J. Stumpf (2007a), An automated technique to quality control radar reflectivity data. *J. Applied Meteorology*, 46 (3), 288–305.
- Lakshmanan, V., T. Smith, G. J. Stumpf, and K. Hondl (2007b), The warning decision support system - integrated information (WDSS-II). *Wea. Forecasting*, 22, No. 3, 592-608.
- Lakshmanan, V., K. Hondl, and R. Rabin (2009), An Efficient, General-Purpose Technique for Identifying Storm Cells in Geospatial Images. *J. Ocean. and Atmos. Tech.*, 26 (3), 523–537.
- Lakshmanan V., and T. Smith (2009), Data Mining Storm Attributes from Spatial Grids. *J. Ocean. and Atmos. Tech.*, In Press
- Larsen, H. R., and E. J. Stansbury (1974), Association of lightning flashes with precipitation cores extending to height 7 km. *J. Atmos. Terr. Phys.*, 36, 1547-1553.
- Lennon, C. L. (1975), LDAR—A new lightning detection and ranging system. *Eos, Trans. Amer. Geophys. Union*, 56, 991.
- MacGorman, D. R., T. Fliaggi, R. L. Holle, and R. A. Brown (2007): Negative Cloud-to-Ground Lightning Flash Raters Relative to VIL, Maximum Reflectivity, Cell Height, and Cell Isolation. *J. of Lightning Res.*, 1, 132-147.
- Maier, L. M., C. Lennon, T. Britt, and S. Schaefer (1995), Lightning Detection and Ranging (LDAR) system performance analysis. Preprints, Sixth Conf. on Aviation Weather Systems, Dallas, TX, Amer. Meteor. Soc., 305-309.
- McNamara, T. M. (2002), The horizontal extent of cloud-to-ground lightning over the Kennedy Space Center. M.S. Thesis, Air Force Institute of Technology, 114 pp.
- Murphy, M. J., K. L. Cummins, N. W. S. Demetriades, and W. P. Roeder (2008), Performance of the New Four-Dimensional Lightning Surveillance System (4DLSS) at the Kennedy Space Center/Cape Canaveral Air Force Station Complex. 13th Conference on Aviation, Range and Aerospace Meteorology, New Orleans, LA. Amer. Meteor. Soc., 20-24 Jan 08, 18 pp.
- Nelson, L. A. (2002), Synthesis of 3-dimensional lightning data and radar to determine the distance that naturally occurring lightning travels from thunderstorms. M.S. Thesis, Air Force Institute of Technology, 85 pp.
- Poehler, H. A., and C. L. Lennon (1979), Lightning Detection and Ranging (LDAR) System Description & Performance Objectives. NASA Technical Memorandum 74106, 86 pp.
- Reynolds, S.E., and M. Brook (1956), Correlation of the Initial Electric Field and the Radar Echo in Thunderstorms. *J. Atmos. Sci.*, 13, 376–380.
- Roeder, W. P., J. T. Madura, and D. E. Harms (2000), Lightning safety for personnel at Cape Canaveral Air Force Station and Kennedy Space Center. Joint Army Navy NASA Air Force / Safety & Environmental Protection Symposium, 8-12 May 00, Cocoa Beach, FL, CPIA Pub 698, 59-70.
- Roeder, W. P., and J. E. Glover (2005), Preliminary results from phase-1 of the statistical forecasting of lightning cessation project. Conference on Meteorological Applications of Lightning Data, 9-13 Jan 05, 6 pp.

- Roeder, W. P., J. W. Weems, and P. B. Wahner (2005), Applications of the Cloud-to-Ground Lightning Surveillance System database. Conf. on Meteorological Applications of Lightning Data, 9-13 Jan 05, 5 pp.
- Stano, G. T., H. E. Fuelberg, and W. P. Roeder (2010), Developing an empirical lightning cessation forecast guidance for the Kennedy Space Center, *J. Geophys. Res.*, in press.
- Vincent, B. R., L. D. Carey, D. Schneider, K. Keeter, R. Gonski (2003), Using WSR-88D reflectivity data for the prediction of cloud-to-ground lightning: A Central North Carolina study. *Nat. Wea. Digest.*, 27, 35-44.
- Vivekanandan, J., S.M. Ellis, R. Oye, D.S. Zrnica, A.V. Ryzhkov, and J. Straka (1999), Cloud Microphysics Retrieval Using S-band Dual-Polarization Radar Measurements. *Bull. Amer. Meteor. Soc.*, 80, 381-388.
- Ward, J. G., K. L. Cummins, E. P. Krider (2008), Comparison of the KSC-ER Cloud-to-Ground Lightning Surveillance System (CGLSS) and the U.S. National Lightning Detection Network (NLDN), 20th International Lightning Detection Conference, 21-23 Apr 2008, Tucson, AZ.
- Weems, J. W., C. S. Pinder, W. P. Roeder, and B. F. Boyd (2001), Lightning watch and warning support to spacelift operations. 18th Conference on Weather Analysis and Forecasting, 30 Jul-2 Aug 01, 301-305.
- Wolf, P. (2006), Anticipating the initiation, cessation, and frequency of cloud-to-ground lightning, utilizing WSR-88D reflectivity data. NOAA / National Weather Service, Jacksonville, Florida.
- Workman, E. J., and S. E. Reynolds (1949), Electrical activity as related to thunderstorm cell growth, *Bull. Am. Meteorol. Soc.*, 30, 142-144.
- Zipser, E.J., and K. Lutz, (1994), The vertical profile of radar reflectivity of convective cells: A strong indicator of storm intensity and lightning probability?, *Mon. Wea. Rev.*, 122, 1751-1759.